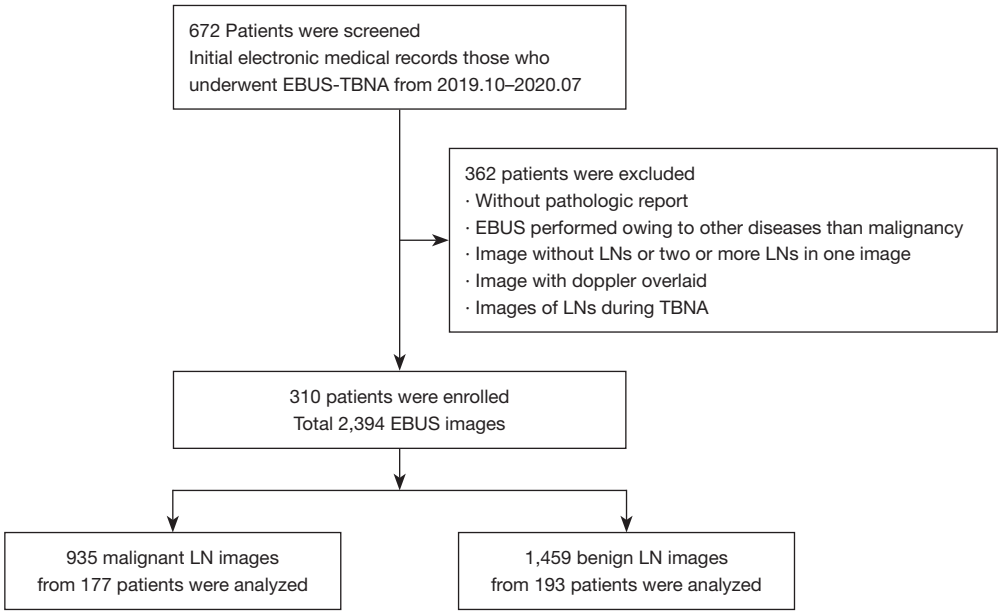

Figure S1 Consort flow diagram. EBUS-TBNA, endobronchial ultrasound-guided transbronchial needle aspiration; LN, lymph node.

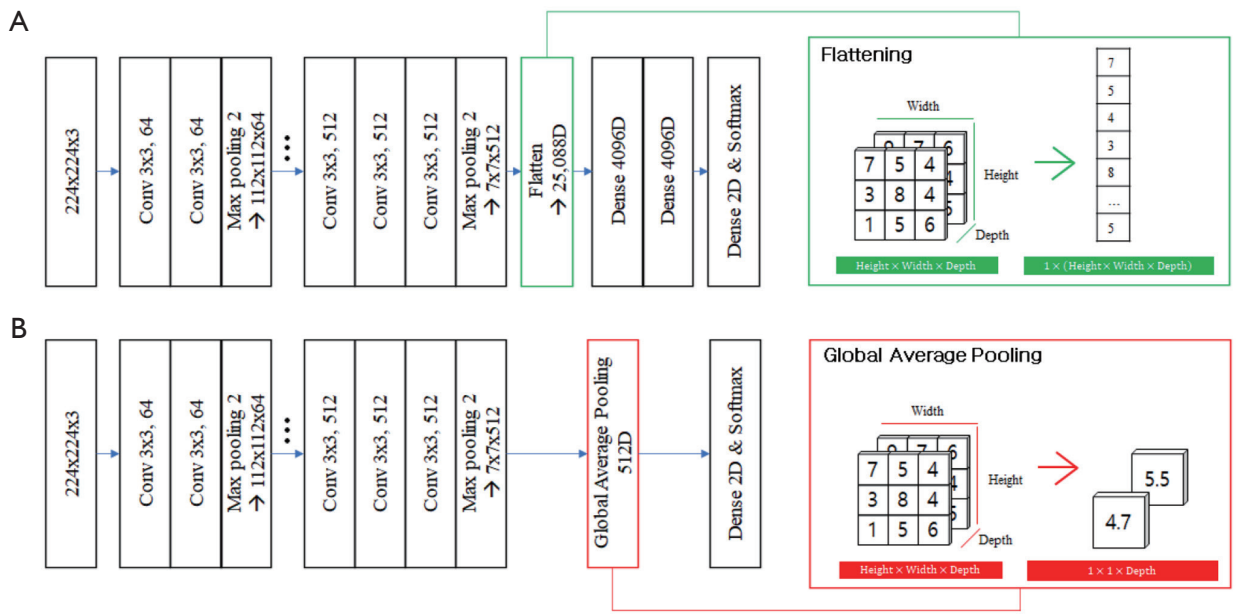

Figure S2 (A) Architecture of the original VGG-16. To flatten the output of the last convolutional layer, all components of the matrix are lined up. (B) Architecture of the VGG-16 with the GAP operation. By calculating the average in the directions of width and height, the global average is fed into the next layer. Conv, convolution; D, dimension; VGG, visual geometry group; GAP, global average pooling.

https://dx.doi.org/10.21037/tlcr-21-870

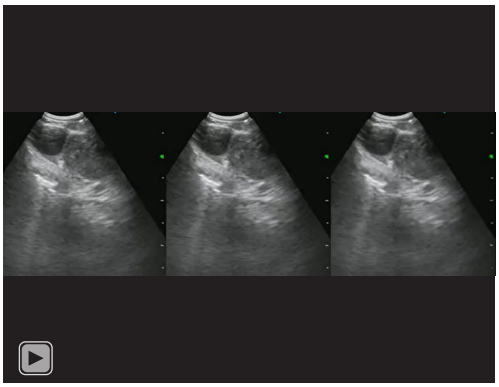

Video S1 Real-time performance of VGG-16 type C. This video was taken during the EBUS-TBNA procedure and demonstrated the performance of the modified VGG-16 (VGG-16 type C) model. M indicates the possibility of malignancy. VGG, visual geometry group; EBUS-TBNA, endobronchial ultrasound-guided transbronchial needle aspiration.

https://dx.doi.org/10.21037/tlcr-21-870

Table S1 Composition of the 3-fold cross-validation dataset

Fold	Training		Validation		Evaluation		Total	
	Images	Patients	Images	Patients	Images	Patients	Images	Patients
Fold 1								
Malignancy	142	732	19	100	16	100	177	932
Benign	161	1,258	13	100	19	100	193	1,458
Fold 2								
Malignancy	144	733	14	100	19	100	177	933
Benign	164	1,258	16	100	13	100	193	1,458
Fold 3								
Malignancy	138	731	21	100	18	100	177	931
Benign	163	1,256	15	100	15	100	193	1,456

Table S2 Malignancy prediction performance of the original VGG-16 (type A), the VGG-16 with global average pooling (type B), the VGG-16 with global average pooling using the proposed loss function (type C), and ResNet

Network	Malignant					Benign					Accuracy	AUC
	TP	FP	FN	Sensitivity	Specificity	TP	FP	FN	Sensitivity	Specificity		
VGG-16 type A												
CV0	71	35	29	0.71	0.65	65	29	35	0.65	0.71	0.680	0.77
CV1	73	21	27	0.73	0.79	79	27	21	0.79	0.73	0.760	0.832
CV2	65	21	35	0.65	0.79	79	35	21	0.79	0.65	0.720	0.737
CV0 + CV1 + CV2	209	77	91	0.6966667	0.743333333	223	91	77	0.74333333	0.69666667	0.720	0.782
VGG-16 type B												
CV0	74	30	26	0.74	0.7	70	26	30	0.7	0.74	0.72	0.792
CV1	72	18	28	0.72	0.82	82	28	18	0.82	0.72	0.77	0.825
CV2	59	34	41	0.59	0.66	66	41	34	0.66	0.59	0.625	0.661
CV0 + CV1 + CV2	205	82	95	0.6833333	0.726666667	218	95	82	0.72666667	0.68333333	0.705	0.759
VGG-16 type C												
CV0	75	25	25	0.75	0.75	75	25	25	0.75	0.75	0.75	0.794
CV1	74	12	26	0.74	0.88	88	26	12	0.88	0.74	0.81	0.848
CV2	69	26	31	0.69	0.74	74	31	26	0.74	0.69	0.715	0.752
CV0 + CV1 + CV2	218	63	82	0.7266667	0.79	237	82	63	0.79	0.72666667	0.758333	0.8
ResNet												
CV0	71	28	29	0.71	0.72	72	29	28	0.72	0.71	0.715	0.737
CV1	63	16	37	0.63	0.84	84	37	16	0.84	0.63	0.735	0.803
CV2	60	23	40	0.6	0.77	77	40	23	0.77	0.6	0.685	0.725
CV0 + CV1 + CV2	194	67	106	0.6466667	0.776666667	233	106	67	0.77666667	0.64666667	0.711667	0.759

Sensitivity = TP/(TP + FN); Specificity = TN/(TN + FP); Accuracy = (TP + TN)/total n. VGG, visual geometry group; ResNet, residual network; TP, true positive; FP, false positive; FN, false negative; AUC, area under the curves; CV, cross validation.

https://dx.doi.org/10.21037/tlcr-21-870

Table S3 Logistic regression analysis for sonographic features to predict malignancy

Sonographic features	Univariate analysis		Multivariate analysis	
	OR (95% CI)	Significance	OR (95% CI)	Significance
Shape				
Oval	1	P<0.001	1	P<0.001
Round	31.5 (13.8–71.9)		28.3 (10.5–76.2)	
Margin				
Indistinct	1	P<0.001	1	P<0.001
Distinct	14.3 (3.3–61.9)		31.1 (5.0–195.0)	
Echogenicity				
Homogeneous	1	P<0.001	1	P=0.005
Heterogeneous	6.9 (3.5–13.5)		3.9 (1.5–10.1)	
Central hilar structure				
Presence	1	P=0.556	1	P=0.068
Absence	1.2 (0.6–2.3)		2.8 (0.9–8.4)	
Coagulation necrosis sign				
Absence	1	P=0.011	1	P=0.462
Presence	5.6 (1.5–21.0)		1.9 (0.3-11.5)	

OR, odds ratio; CI, confidence interval.

https://dx.doi.org/10.21037/tlcr-21-870